No. 68-73

A DOUBLET LATTICE METHOD FOR CALCULATING LIFT DISTRIBUTIONS ON OSCILLATING SURFACES IN SUBSONIC FLOWS

by

E. ALBANO and W. P. RODDEN
Northrop/Norair
Hawthorne, California

AIAA Paper
No. 68-73

AIAA 6th Aerospace Sciences Meeting

NEW YORK, NEW YORK/JANUARY 22-24, 1968

A DOUBLET LATTICE METHOD FOR CALCULATING LIFT DISTRIBUTIONS ON OSCILLATING SURFACES IN SUBSONIC FLOWS

E. Albano, Senior Engineer
W. P. Rodden, Consulting Engineer
Northrop Corporation, Norair Division
Hawthorne, California

Summary

Approximate solutions from the linearized formulation are obtained by simulating the surface by a set of lifting elements which are short line-segments of acceleration potential doublets. The normal velocity induced by an element of unit strength is given by an integral of the subsonic kernel function. The load on each element is determined by satisfying normal velocity boundary conditions at a set of points on the surface. It is seen a posteriori that the lifting elements and collocation stations can be located such that the Kutta condition is satisfied approximately. The method obviates the prescription of singularities in lift distribution along lines where normal velocity is discontinuous, and is readily adapted for problems of complex geometries. Results compare closely with those from methods which prescribe lift-mode series, and from pressure measurements. The technique constitutes an extension of a method developed by S. G. Hedman for steady flow.*

Symbols

AR	Aspect ratio
b	Semichord
c	Chord
K	Kernel function
k	Reduced frequency $k = \omega b/U$
M	Free stream Mach number
NC	Number of boxes on a chord
NS	Number of boxes on semispan
$p\cdot(\frac{1}{2}\rho U^2)$	Complex amplitude of lifting pressure
wU	Complex amplitude of normal velocity at surface
t	Time
x,s	Coordinates on the surface
x,y,z	Cartesian coordinates
ω	Frequency of oscillation
ρ	Free stream density

Introduction

The linearized formulation of the oscillatory subsonic lifting surface theory relates the normal velocity at the surface

$$W(x,s,t) = \mathrm{Re}\left\{\bar{w}(x,s)\, e^{i\omega t}\right\}$$

to the pressure difference across the surface

$$P(x,s,t) = \mathrm{Re}\left\{\bar{p}(x,s)\, e^{i\omega t}\right\}$$

by a singular integral equation and the Kutta condition at the trailing edge (TE):

$$\frac{\bar{w}(x,s)}{U} = \frac{1}{4\pi\rho U^2} \iint_S K(x,\xi,s,\sigma;\omega,M)\bar{p}(\xi,\sigma)\, d\xi d\sigma \quad (1)$$

$$\bar{p}\left(x_{TE}(s)\ ,\ s\right) = 0 \quad (2)$$

where (x,s) are orthogonal coordinates on the surface S such that the undisturbed stream is directed parallel to the x-axis.

Rodemich[1] has given a derivation of the kernel function for a nonplanar surface, and Landahl[2] has presented a relatively concise formula:

$$K = e^{-i\omega x_0/U}(K_1T_1 + K_2T_2)/r_1^2 \quad (3)$$

where

$$T_1 = \cos\left[\gamma(s) - \gamma(\sigma)\right]$$

$$T_2 = \left[z_o \cos\gamma(s) - y_o \sin\gamma(s)\right] \times \left[z_o \cos\gamma(\sigma) - y_o \sin\gamma(\sigma)\right] / r_1^2$$

$$K_1 = I_1 + Mr_1 e^{-ik_1u_1}/R(1 + u_1^2)^{\frac{1}{2}}$$

$$K_2 = -3I_2 - ik_1M^2r_1^2\, e^{-ik_1u_1}/R^2(1 + u_1^2)^{\frac{1}{2}} - \frac{Mr_1}{R}\left[(1 + u_1^2)\frac{\beta^2r_1^2}{R^2} + 2 + \frac{Mr_1u_1}{R}\right]\frac{e^{-ik_1u_1}}{(1+u_1^2)^{3/2}}$$

$$I_1 = \int_{u_1}^{\infty}\frac{e^{-ik_1u}}{(1 + u^2)^{3/2}}\, du\ ,\quad I_2 = \int_{u_1}^{\infty}\frac{e^{-ik_1u}}{(1 + u^2)^{5/2}}\, du$$

$$x_o = x - \xi\ ,\qquad y_o = y - \eta\ ,\qquad z_o = z - \zeta$$

$$r_1 = (y_o^2 + z_o^2)^{\frac{1}{2}},\qquad R = (x_o^2 + \beta^2r_1^2)^{\frac{1}{2}}$$

$$u_1 = (MR - x_o)/\beta^2r_1,\quad k_1 = \omega r_1/U,\quad \beta = (1 - M^2)^{\frac{1}{2}} \quad (4)$$

---

*At the time of this writing, the authors learned that a similar extension had been developed independently by Stark.[19]

The coordinate system is illustrated in Fig. 1. The symbol $⨍$ means that the integral in Eq. (1) is defined in the "finite part" sense[3].

The traditional method for obtaining approximate solutions for $\bar{p}$ when $\bar{w}$ is given is to assume a series approximation

$$\bar{p} \approx \sum_i \sum_j a_{ij} \, f_i(x) \, g_j(s)$$

and to determine the coefficients a_{ij} by satisfying normal-velocity conditions on the surface. Known properties of the force distribution $\bar{p}$ such as the behavior near surface edges are built into the approximation by appropriate choice of the functions in the series. This technique has been used successfully for at least ten years, although most applications have been for planar wings without control surfaces.

Consideration of the efforts needed to develop a single computer program to handle a fairly general class of nonplanar problems has led us to seek a technique which would obviate the prescription of the behavior of $\bar{p}$ along edges and corners and in fact, would remove a priori restrictions on the global behavior of the force distribution. The "box methods" for the supersonic problem provide examples of the methods sought.

Doublet-Lattice Method

We describe a method which is an extension of the one developed for steady subsonic flow by Hedman[4] in 1965. The elements of the technique are to be found in the vortex-lattice method of Falkner[5]. Since it appears at the present time that a rigorous analytical basis for the method is not available, we present an operational description:

It is assumed that the surface can be approximated by segments of planes. The surface is divided into small trapezoidal panels ("boxes") in a manner such that the boxes are arranged in columns parallel to the free stream (Fig. 2), and so that surface edges, fold lines and hinge lines lie on or near box boundaries. The 1/4-chord line of each box is taken to contain a distribution of acceleration potential doublets of uniform but unknown strength. In steady flow, each doublet line-segment will be equivalent to a velocity-potential horseshoe vortex whose "bound" portion coincides with the doublet line.

Let n be the number of boxes and let the doublet strength in the j^{th} line segment be

$$\bar{f}_j \quad d\mu \, / 4\pi\rho$$

where $\bar{f}_j$ is the complex amplitude of the force per unit length along the line, and $d\mu$ the incremental length. The normal velocity (downwash) induced at a point (x_i, s_i) on the surface is

$$\begin{aligned} w_i &= \bar{w}(x_i, s_i)/U \\ &= \sum_{j=1}^{n} \frac{\bar{f}_j}{4\pi\rho U^2} ⨍_{\ell_j} K\big(x_i, s_i, x_j(\mu), s_j(\mu)\big)\, d\mu \end{aligned} \tag{5}$$

where each integration runs along the line segment whose length is ℓ_j. If Eq. (5) is applied at n downwash points on the surface, the $\bar{f}_j$ are determined. The force on the doublet line is taken as the force on the box and the pressure difference across the surface is approximated by

$$\begin{aligned} \bar{p}_j &= \text{force/(box area)} = \bar{f}_j \ell_j/\text{(box area)} \\ &= \bar{f}_j / (\bar{x}_j \cos \lambda_j) \end{aligned} \tag{6}$$

where $\bar{x}_j$ is the box average chord and λ_j the sweep angle of the doublet line.

We note that the induced downwash calculated by Eq. (5) will be infinite if the downwash point lies on a doublet line segment or downstream from its end points. Furthermore, the Kutta condition has not been imposed.

From numerical experimentation with this technique, it has become apparent that the Kutta condition will be satisfied approximately if each downwash point is the point at midspan and 3/4-chord of a box.

Eq. (5) is written

$$w_i = \sum_{j=1}^{n} D_{ij} \, p_j \tag{7}$$

where

$$\begin{aligned} p &= \bar{p} / \tfrac{1}{2} \rho U^2 \\ D_{ij} &= \frac{1}{8\pi} \; \bar{x}_j \cos \lambda_j ⨍_{\ell_j} K\big(x_i, s_i, x_j(\mu), s_j(\mu)\big)\, d\mu \end{aligned} \tag{8}$$

If A_{ij} are the elements of the matrix whose inverse is the matrix of D_{ij}, then

$$p_i = \sum_{j=1}^{n} A_{ij} \, w_j \tag{9}$$

provides the approximate solution for the force distribution.

Generalized force coefficients are computed approximately by

$$Q_{ij} = \frac{1}{b^3} \sum_{k=1}^{n} h_k^{\,i} \, p_k^{\,j} \, S_k \tag{10}$$

where

S_k = area of box k

$h_k^{\,i}$ = deflection in mode i of 1/4 chord, mid-span point of box k

$p_k^{\,j}$ = force distribution in mode j at box k

b = reference length

Working Forms

Approximate evaluation of the integral in Eq. (8) is achieved by approximating the integrand by a simple function. We consider the downwash induced at a receiving point $R = (x_R, y_R, z_R)$ by a doublet line segment whose end points are S_- and S_+ and whose midpoint is S_o. Let

$$\bar{K} = r_1^{\,2} K \tag{11}$$

Denote

$$\bar{K}_o = \bar{K}(R,S_o) = \bar{K}(x_R, y_R, z_R, x_{S_o}, y_{S_o}, z_{S_o}; \omega, M)$$
$$\bar{K}_+ = \bar{K}(R,S_+)$$
$$\bar{K}_- = \bar{K}(R,S_-)$$

Define the coordinate system (Fig. 3)

$$\begin{aligned} \eta &= y \cos\gamma_\sigma - z \sin\gamma_\sigma \\ \zeta &= -y \sin\gamma_\sigma + z \cos\gamma_\sigma \end{aligned} \tag{12}$$

Since the length of the doublet segment is small, it may be expected that a parabolic approximation for $\bar{K}$ along the segment would be sufficient in evaluating the integral.

$$\begin{aligned} I_{ij} &= \oint_{\ell_i} K(x_i, s_i, x_j(\mu), s_j(\mu); \omega, M) \cos\lambda_j \, d\mu \\ &\approx \oint_{-e}^{e} \frac{A\bar{\eta}^2 + B\bar{\eta} + C}{(\eta_o - \bar{\eta})^2 + \zeta_o^{\,2}} \, d\bar{\eta} \end{aligned} \tag{13}$$

where

$$e = \frac{1}{2} \ell_j \cos\lambda_j$$
$$\eta_o = (y_R - y_{So}) \cos\gamma_\sigma + (z_R - z_{So}) \sin\gamma_\sigma$$
$$\zeta_o = -(y_R - y_{So}) \sin\gamma_\sigma + (z_R - z_{So}) \cos\gamma_\sigma$$
$$A = (\bar{K}_+ - 2\bar{K}_o + \bar{K}_-)/2e^2$$
$$B = (\bar{K}_+ - \bar{K}_-)/2e$$
$$C = \bar{K}_o$$

The result of the integration is

$$\begin{aligned} I_{ij} \approx \left[(\eta_o^{\,2} - \zeta_o^{\,2})A + \eta_o B + C\right] \cdot |\zeta_o|^{-1} \tan^{-1}\left(\frac{2e|\zeta_o|}{r_1^{\,2} - e^2}\right) \\ + \left(\frac{1}{2} B + \eta_o A\right) \log \frac{r_1^{\,2} - 2\eta_o e + e^2}{r_1^{\,2} + 2\eta_o e + e^2} + 2eA \end{aligned} \tag{15}$$

where

$$r_1^{\,2} = \eta_o^{\,2} + \zeta_o^{\,2}$$

For the planar case ($\zeta_o \to 0$)

$$\begin{aligned} I_{ij} = (\eta_o^{\,2} A + \eta_o B + C)\left(\frac{1}{\eta_o - e} - \frac{1}{\eta_o + e}\right) \\ + \left(\frac{1}{2} B + \eta_o A\right) \log\left(\frac{\eta_o - e}{\eta_o + e}\right)^2 + 2eA \end{aligned}$$

In order to converge to Hedman's vortex lattice results for steady flow and to improve the approximation of Eq. (15), we have found it convenient to subtract the steady part ($\omega = 0$) from $\bar{K}$ before applying the above formulas, and then to add the effect of a horseshoe vortex.

Approximate evaluation of the integrals I_1 and I_2 in the kernel function may be accomplished in many ways. L. Schwarz[6] has given an expression for I_1 in terms of infinite series. However, we choose to approximate the integrands by simple functions. It is sufficient to consider nonnegative arguments because of symmetry properties of the integrand. Integration by parts gives

$$\begin{aligned} I_1(u_1; k_1) &= \int_{u_1}^{\infty} \frac{e^{-ik_1 u}}{(1+u^2)^{3/2}} \, du \\ &= \left(1 - \frac{u_1}{\sqrt{1+u_1^{\,2}}}\right) e^{-ik_1 u_1} - ik_1 \int_{u_1}^{\infty} \left(1 - \frac{u}{\sqrt{1+u^2}}\right) e^{-ik_1 u} \, du \end{aligned}$$

Watkins[7] has given the formula

$$\begin{aligned} t/\sqrt{1+t^2} \approx 1 &- 0.101 \exp(-0.329t) \\ &- 0.899 \exp(-1.4067t) \\ &- 0.09480933 \exp(-2.90t) \sin \pi t, \qquad (t \geq 0) \end{aligned}$$

which when substituted in the above yields a simple expression for I_1. The integral I_2 is approximated in similar fashion.

In view of the lack of a rigorous basis for the foregoing assumptions, it is necessary to demonstrate the adequacy of the doublet lattice method by comparison of results with solutions obtained by other means, and with experimental data.

Results for Two-Dimensional Flow

For planar flow the integral equation (1) becomes the one-dimensional integral equation of Possio (see, e.g., section 6-4 of Ref. 8) and the doublet line segments become doublets on the chord. The results of the doublet lattice method presented here have been obtained by dividing the airfoil chord into equal intervals and taking a sending and receiving point at the 1/4-chord and 3/4-chord, respectively, of each interval.

Exact solutions are available for incompressible flow. Solutions for an airfoil with oscillating flap are compared in Fig. 4, where measurements reported by Bergh[9] are included.

The doublet lattice method may be thought of as producing step-function approximations to the pressure distribution. Rather than present these in graphs, we have chosen to draw curves through the values for p at sending points. Also in describing results, we use the term "boxes" to mean intervals (in 2-D flow) or small panels (in 3-D flow), and

NC = Number of boxes per wing chord

NS = Number of boxes per semi-span (planar wings)

The table below is a comparison of generalized forces from the present method and from the tables of Ref. 10. The coefficients are defined by

$$L = \pi \rho U^2 \ b \ e^{ikt}(Ak_a + Bk_b + Ck_c)$$

$$M = \pi \rho U^2 \ b \ e^{ikt}(Am_a + Bm_b + Cm_c)$$

$$N = \pi \rho U^2 \ b \ e^{ikt}(An_a + Bn_b + Cn_c)$$

where b is the semichord, k the reduced frequency based on b and

L = Force of airfoil and flap, positive downward

M = Moment of wing and flap about midchord, positive tail heavy

N = Moment of flap about hinge axis, positive tail heavy

Ab = Translation amplitude, positive downward

B = Amplitude of airfoil rotation about midchord, positive trailing edge down

C = Amplitude of flap rotation, positive trailing edge down

Results shown here are for the case $M = 0.8$, $k = 0.9$, $\tau = $ (flap chord)/(airfoil chord) $= 0.3$.

The tabulated results indicate that the doublet lattice approximation would be valid for high subsonic Mach numbers and reduced frequencies of order unity.

Results for Three-Dimensional Flows

Fig. 5 compares calculated lift distributions with measurements reported in NACA RM A51G31 for a swept, tapered wing at incidence in steady flow. For this problem, the semi-wing was divided into 48 boxes, each containing a horseshoe vortex as in Hedman's method. Results for the wing stations shown were obtained by interpolation.

Calculations and measurements for a wing with partial-span flap are presented in Fig. 6. The curves labeled "experiment" were obtained by reduction of graphical data of Ref. 12 and for this reason, are rather imprecise. Calculations were made with eighty horseshoe vortices on the semi-wing, eight vortices being on the flap. Landahl[13] has shown that both the form and strength of the pressure singularity at the hinge line can be determined analytically. The expression for the lift distribution for unit flap angle is:

$$p = \frac{-2}{\pi \beta_n} \cos \lambda_c \ \log \left| \frac{x - x_c}{c} \right| + O(1) \qquad (16)$$

	20 "boxes"	30 "boxes"	Reference 10
k_a	-0.0075 -1.118 i	-0.0197 -1.119 i	-0.0444 -1.1201i
k_b	-1.571 -0.0921i	-1.574 -0.0795i	-1.5755 -0.0267i
k_c	-0.4835 +0.0789i	-0.4824 +0.0823i	-0.4803 +0.0868i
m_a	0.3293 +0.1005i	0.3303 +0.0924i	0.3309 +0.0760i
m_b	-0.0391 -0.8604i	-0.0572 -0.8623i	-0.0946 -0.8619i
m_c	-0.4075 +0.0021i	-0.4105 +0.0058i	-0.4147 +0.0248i
n_a	0.0584 -0.0626i	0.0591 -0.0638i	0.06012 -0.06609i
n_b	-0.0745 -0.1456i	-0.0762 -0.1474i	-0.0798 -0.1504i
n_c	-0.0912 -0.0696i	-0.0919 -0.0712i	-0.0931 -0.0739i

where

x_c = coordinate of hinge

λ_c = hingeline sweep angle

$\beta_n = \sqrt{1 - M^2 \cos^2 \lambda_c}$

c = local chord

For the wing considered here, $\lambda_c \doteq 30°$, $M = 0.6$; the singular part of Eq. (16) becomes

$$p \approx 1.20 \log \left| \frac{x - x_c}{c} \right| \tag{16a}$$

The graph of this expression is labeled "local solution" in Fig. 6a. Fig. 6b shows the distribution of lift on the semi-wing calculated by the horseshoe vortex lattice technique.

Both kernel function calculations and measurements of lift distribution reported in NASA TN D-344 are compared in Fig. 7 with results from the doublet lattice method. The Æ3 rectangular wing considered is oscillating in a bending mode described approximately by

$$\bar{h} \approx 0.18043|\bar{y}| + 1.70255\bar{y}^2 - 1.13688|\bar{y}^3| + 0.25387\bar{y}^4$$

where $\bar{h}$ is the nondimensional deflection amplitude, $\bar{y}$ the nondimensional spanwise coordinate based on the semispan.

Results of computations for an aspect ratio 2 rectangular wing with full span 40% chord oscillating flap are shown in Fig. 8. These are compared with kernel function calculations (with built-in hingeline singularity) given in reference 15, and experimental data of reference 16. The doublet-lattice calculations were made with 99 boxes on the semi-wing and of these, 45 boxes were on the flap.

Some preliminary results of computations for a rectangular T-tail are presented in Fig. 9, where measurements by Clevenson and Leadbetter[17] are reproduced. To account in part for the tunnel wall, the image system of the fin was included in the calculations; the image of the horizontal stabilizer was neglected. Forty boxes were placed on the fin and forty on the horizontal stabilizer semi-wing. The discrepancy between calculations and experimental data for increasing reduced frequency might be due to the relatively small number of boxes used, or to the incomplete modelling of the effect of the tunnel wall. The T-tail results illustrate that nonplanar problems are easily approached by the doublet lattice technique.

Conclusions

Within the context of the linearized subsonic lifting surface theory, two types of approximations are involved in the doublet lattice method. The assumption that for purposes of calculating lift distributions the surface can be represented by a system of line segments of acceleration potential doublets is seen to be a valid approximation in view of the results obtained. As far as the authors are aware, an analytical basis for this approximation has not been established and certainly deserves to be studied so that its full implications may be brought out. The second kind of approximation is concerned with the evaluation of integrals in the kernel and in the downwash-pressure influence coefficients, Eq. (8). These procedures may be improved and optimized according to the standard techniques of numerical quadrature.

The advantages of the doublet lattice method arise from being able to disregard the special behavior of the lift distribution where the normalwash is discontinuous. So long as edges do not intersect boxes, a computer program based on this technique does not need to discriminate among side edges, fold lines, hinge lines, etc., and this fact is important when problems of intersecting surfaces are considered. Furthermore, since the influence coefficients D_{ij} are independent of the properties of the normalwash distribution, the same matrix computed for a given wing will yield solutions for a large class of normalwash distributions. For example, generalized forces for many different control surface configurations may be obtained from the same influence coefficient matrix.

For applications in aeroelastic analyses, aerodynamic influence coefficients that relate control point forces to deflections have been defined in Ref. 18. The doublet lattice method leads immediately to this definition of influence coefficients since the control point force is given by the product of lifting pressure and box area, and the downwash is the substantial derivative in the streamwise direction of the deflection. (The substantial derivative requires curve fitting "in-the-small" along the surface strip; e.g., a parabola may be passed through the control point and the points upstream and downstream of it.) If a reduced number of degrees of freedom is desired for the aeroelastic analysis over the number of boxes employed in the aerodynamic analysis, the number of control point forces and deflections may be reduced by a streamwise curve fit and the method of virtual work as discussed in Ref. 18.

References

1. Vivian, H. T., and Andrew, L. V., "Unsteady aerodynamics for advanced configurations. Part I - Application of the subsonic kernel function to nonplanar lifting surfaces," Air Force Flight Dynamics Lab. Report FDL-TDR-64-152, Part I (May 1965).

2. Landahl, M. T., "Kernel function for nonplanar oscillating surfaces in a subsonic flow," AIAA J. 5, 1045-1046 (May 1967).

3. Mangler, K. W., "Improper integrals in theoretical aerodynamics," British A.R.C. R&M 2424 (1951).

4. Hedman, S. G., "Vortex lattice method for calculation of quasisteady-state loadings on thin elastic wings," Aeronautical Research Institute of Sweden Report 105 (October 1965).

5. Falkner, V. M., "The calculation of aerodynamic loading on surfaces of any shape," British A.R.C. R&M 1910 (1943).

6. Schwarz, L., "Investigation of some functions related to the cylinder functions of zero order," Luftfahrtforshung, Vol. 20, No. 12, 341-372 (1944).

7. Watkins, C. E., Runyan, H. L., and Cunningham, H. J., "A systematic kernel function procedure for determining aerodynamic forces on oscillating or steady finite wings at subsonic speeds," NASA Tech. Report R-48 (1959).

8. Bisplinghoff, R. L., Ashley, H., and Halfman, R. L., Aeroelasticity (Addison Wesley, New York, 1957) Chap. VI, p. 294.

9. Bergh, H., "A new method for measuring the pressure distribution on harmonically oscillating wings of arbitrary planform," National Aeronautical and Astronautical Research Institute, Amsterdam, Report MP.224 (1964).

10. Anon., "Tables of aerodynamic coefficients for an oscillating wing-flap system in a subsonic compressible flow," National Aeronautical and Astronautical Research Institute, Amsterdam, Report F.151 (May 1954).

11. Kolbe, C. D., and Boltz, F. W., "The forces and pressure distribution at subsonic speeds on a plane wing having 40° of sweepback, an aspect ratio of 3, and a taper ratio of 0.5," NACA RM A51G31 (1951).

12. Hammond, A. D., and Keffer, B. M., "The effect at high subsonic speeds of a flap-type aileron on the chordwise pressure distribution near midsemi-span of a tapered 35° sweptback wing of aspect ratio 4 having NACA 65A006 section," NACA RM L53C23 (1953).

13. Landahl, M. T., "On the pressure loading functions for oscillating wings with control surfaces," Proceedings of the AIAA/ASME 8th Structures, Structural Dynamics and Materials Conference, 142-147 (March 1967).

14. Lessing, H. C., Troutman, J. L., and Menees, G. P., Experimental determination of the pressure distribution on a rectangular wing oscillating in the first bending mode for Mach numbers from 0.24 to 1.30," NASA TN D-344 (1960).

15. Curtis, A. R., Gikas, X. A., and Hassig, H. J., "Oscillatory flap aerodynamics - comparison between theory and experiment," Paper presented at the Aerospace Flutter and Dynamics Council Meeting, Cocoa Beach, Florida (Nov. 1967).

16. Beals, V. and Targoff, W. P., "Control surface oscillatory coefficients measured on low-aspect ratio wings," Wright Air Development Center Technical Report No. 53-64 (April 1953).

17. Clevenson, S. A., and Leadbetter, S. A., "Measurements of aerodynamic forces and moments at subsonic speeds on a simplified T-tail oscillating in yaw about the fin mid-chord," NACA Tech. Note 4402 (1958).

18. Rodden, W. P., and Revell. J. D., "The status of unsteady aerodynamic influence coefficients," IAS Fairchild Fund Paper No. FF-33 (1962).

19. Stark, V. J. E., Private communication to W. P. Rodden, 11 Oct. 1967.

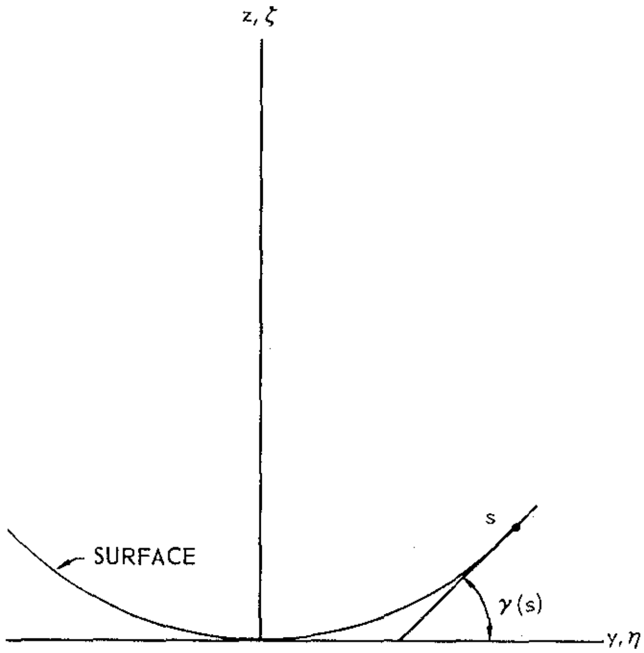

FIGURE 1. COORDINATE SYSTEM

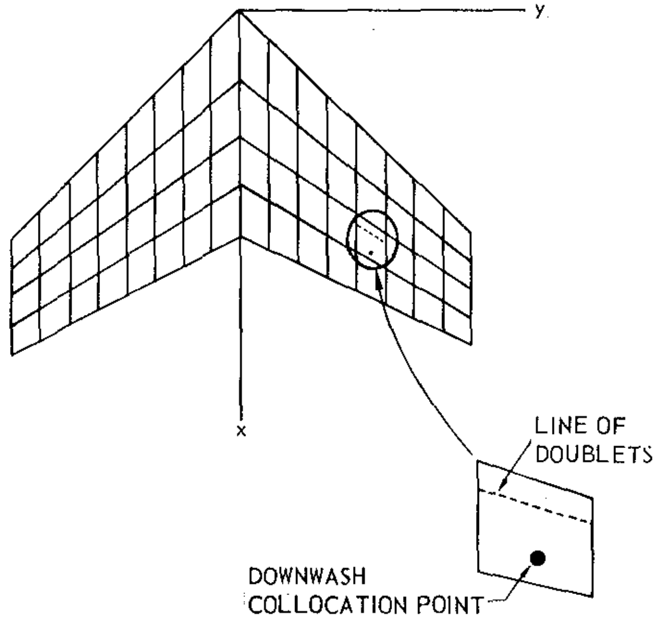

FIGURE 2. WING AND PANEL GEOMETRY

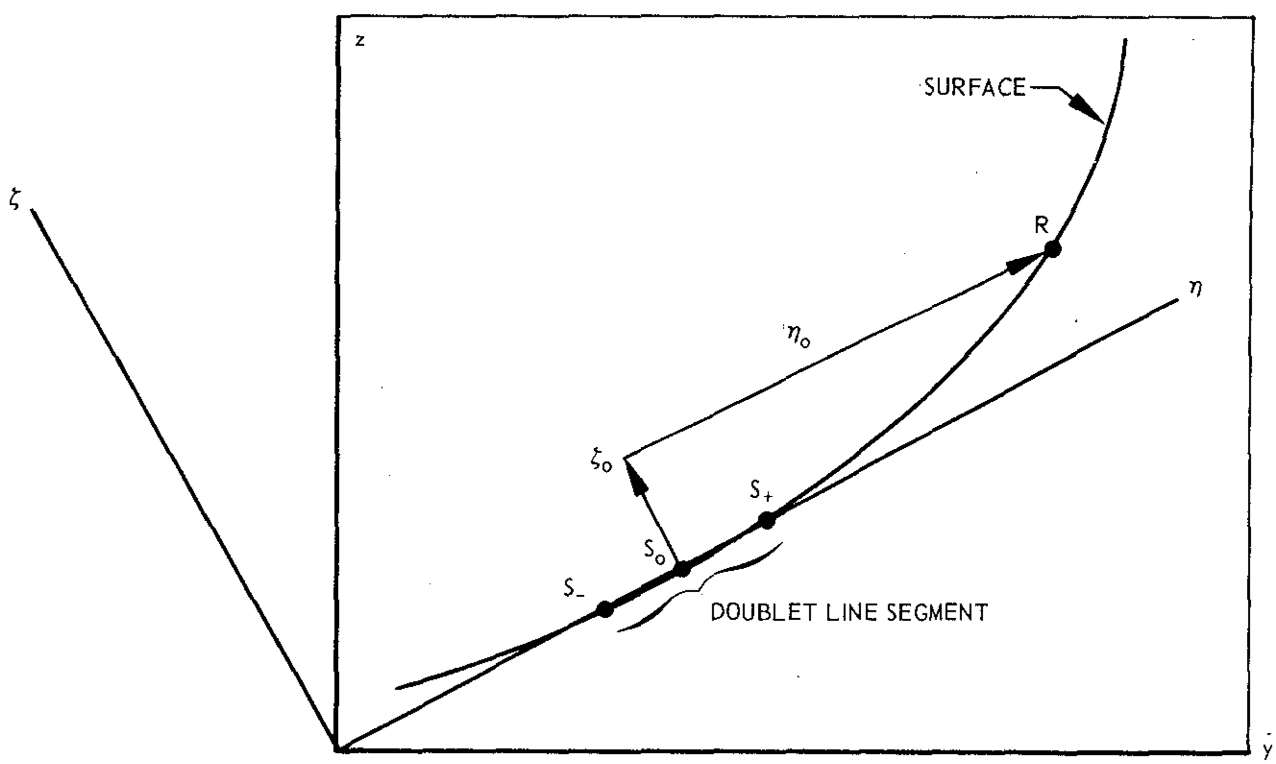

FIGURE 3. COORDINATE SYSTEM OF EQUATION (12).

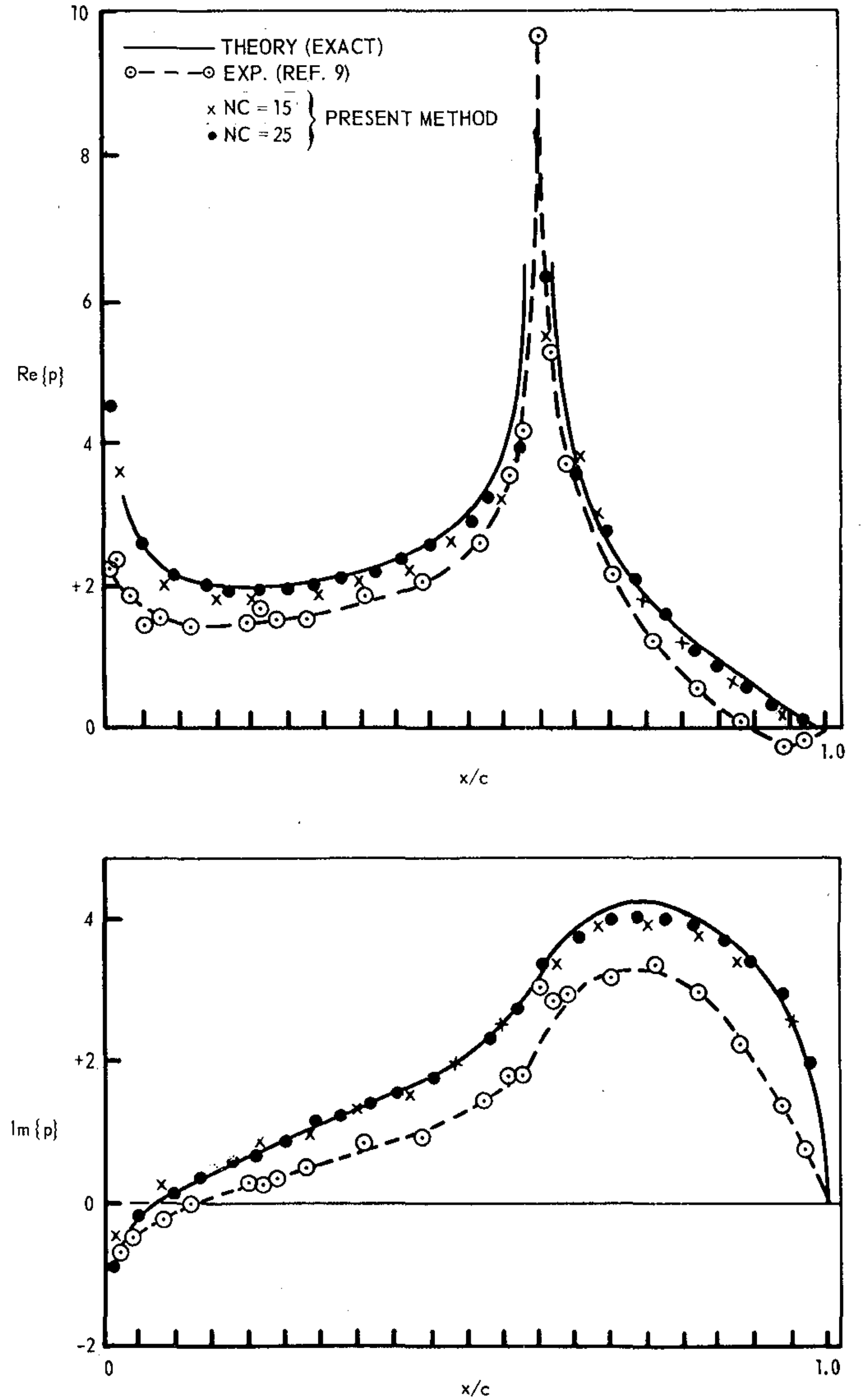

FIGURE 4. LIFTING PRESSURE DISTRIBUTION ON WING WITH OSCILLATING FLAP IN 2D FLOW. M = 0 K = 1.0

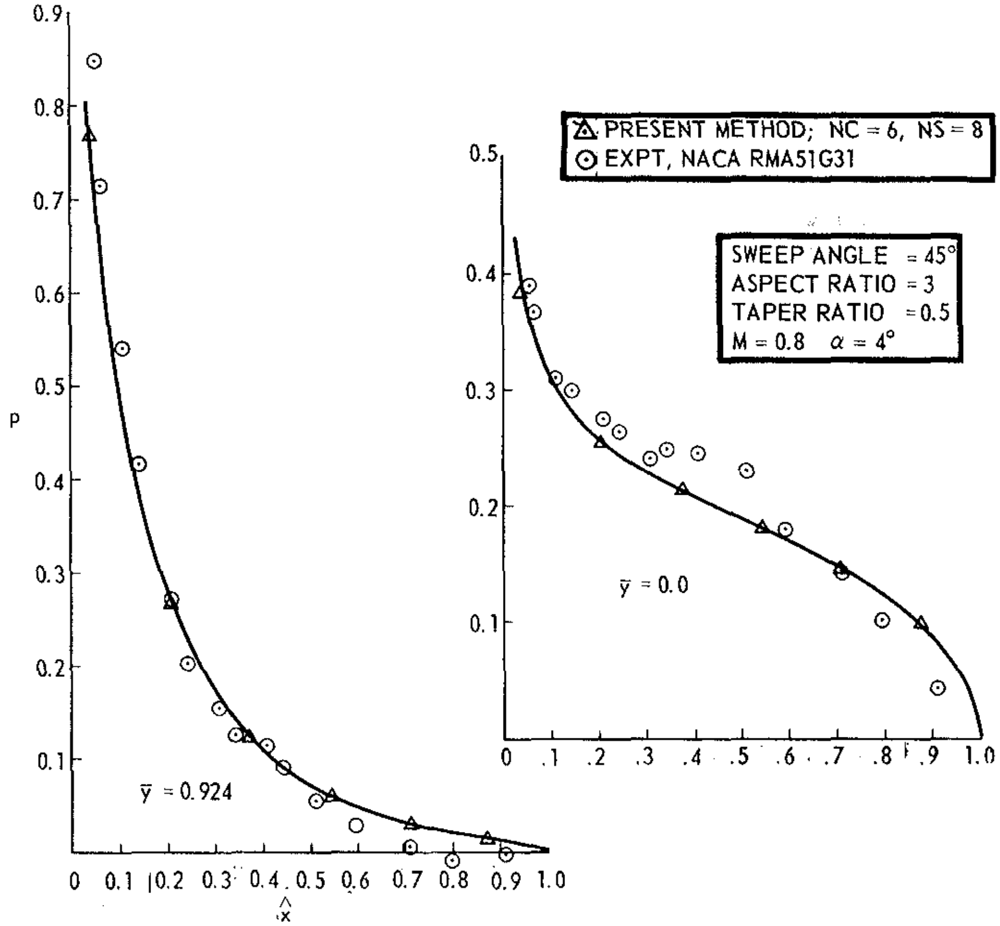

FIGURE 5. LIFT DISTRIBUTION ON SWEPT WING IN STEADY FLOW

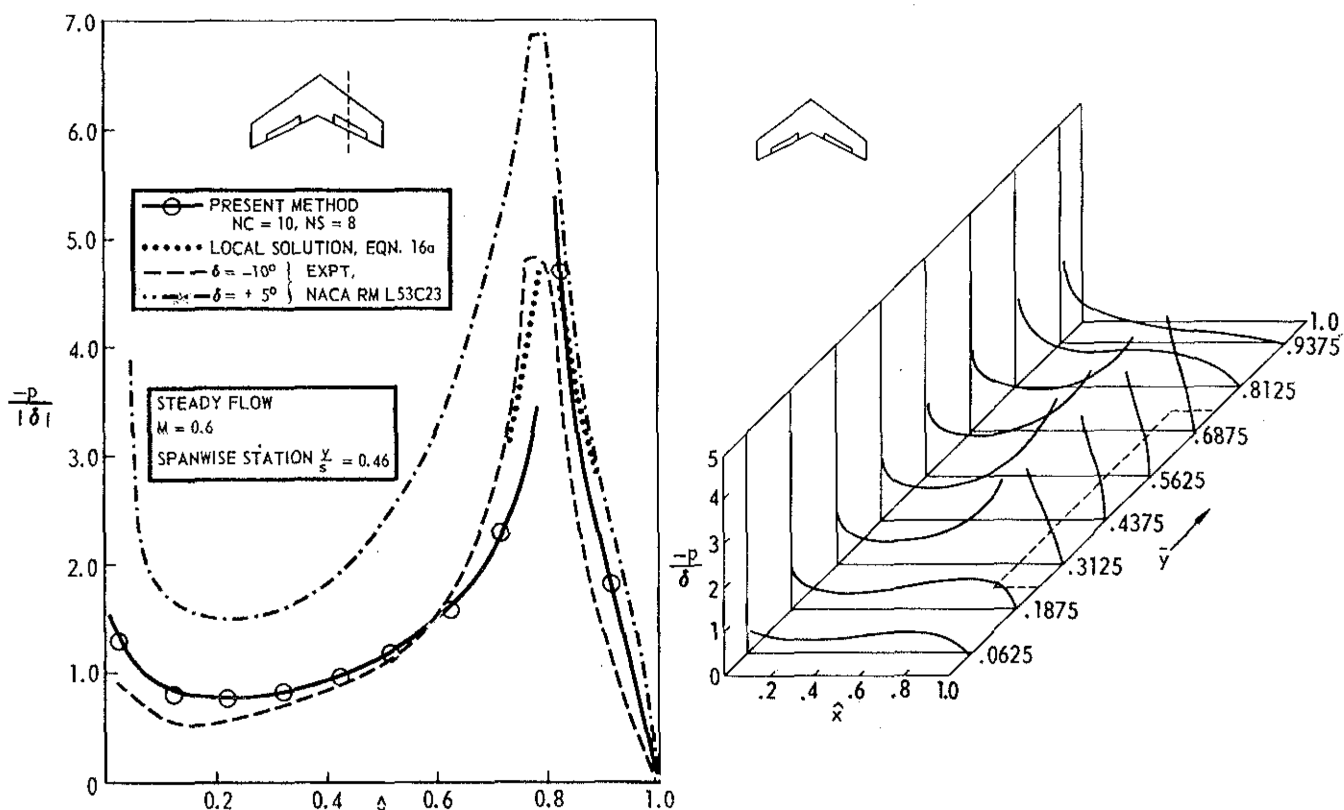

(a) COMPARISON WITH EXPERIMENT (b) CALCULATED LIFT DISTRIBUTION ON SEMIWING

FIGURE 6. LIFT DISTRIBUTION DUE TO DEFLECTED PARTIAL-SPAN FLAP

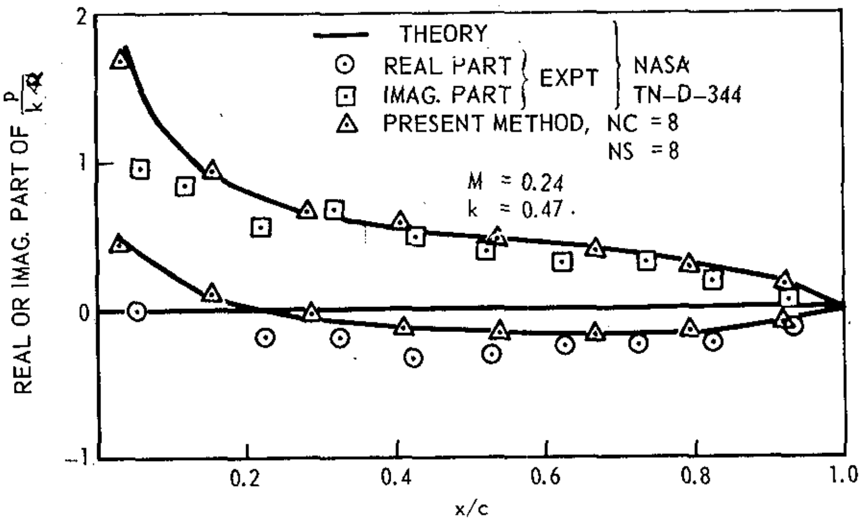

FIGURE 7. LIFT DISTRIBUTION ON $\mathcal{R}$3 RECTANGULAR WING OSCILLATING IN BENDING MODE (a) $\frac{y}{s} = 0$

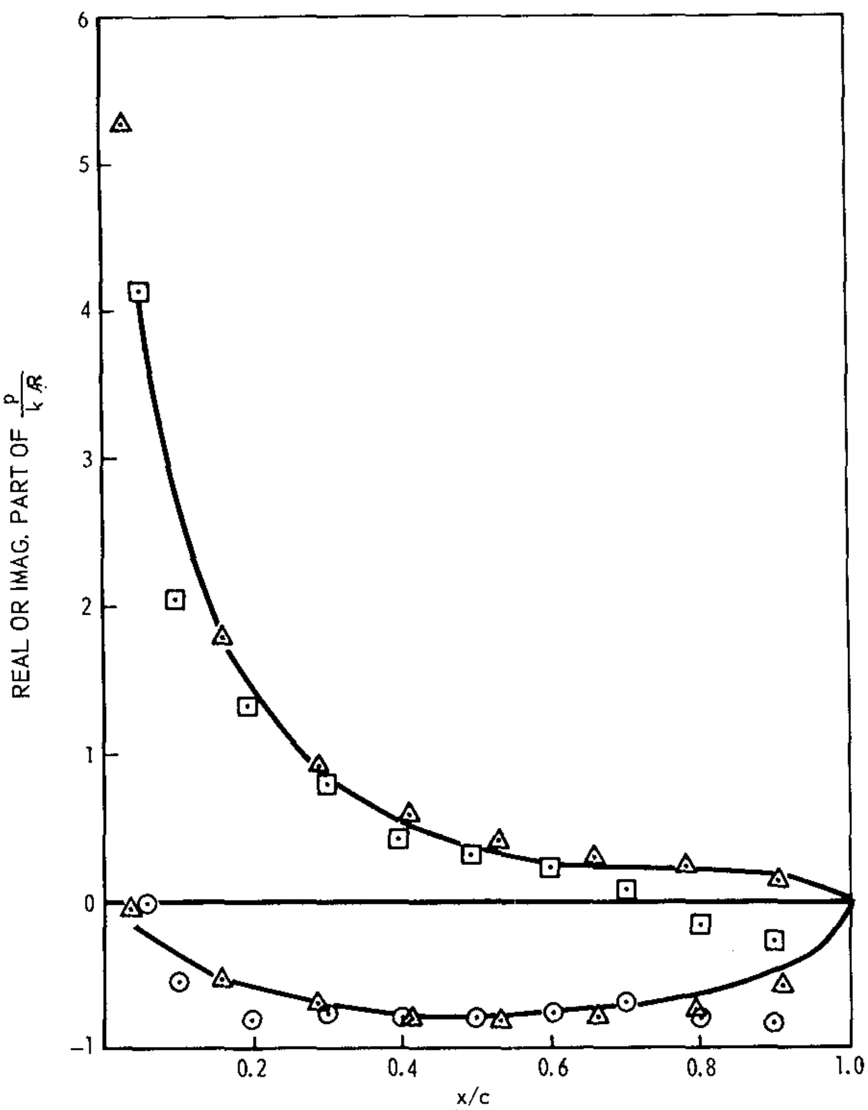

FIGURE 7. CONTINUED. (b) $\frac{y}{s} = 0.9$

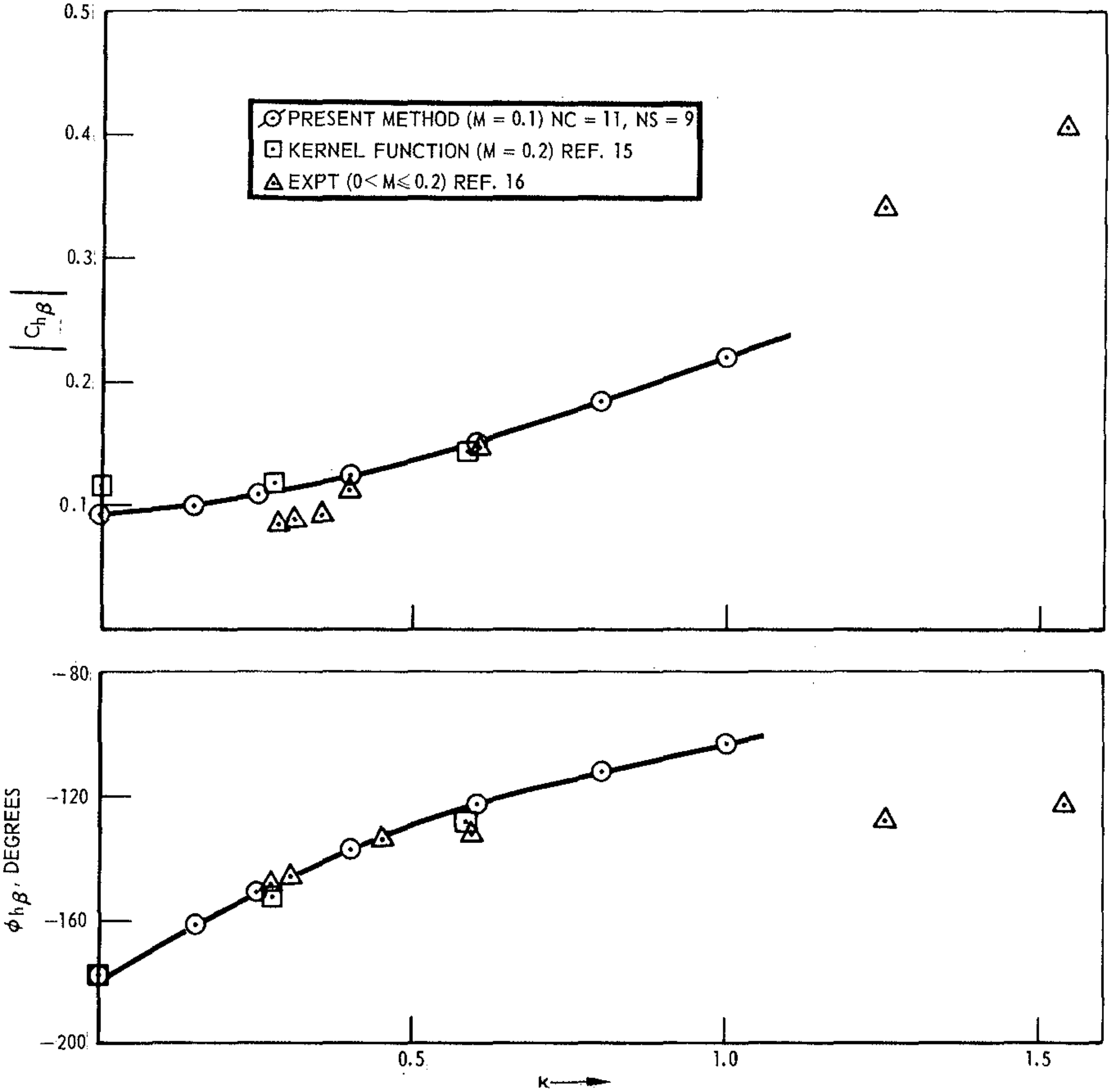

FIGURE 8. FLAP HINGE MOMENT DUE TO FLAP OSCILLATION, FOR A 40% CHORD, FULL SPAN FLAP ON AR 2 RECTANGULAR WING

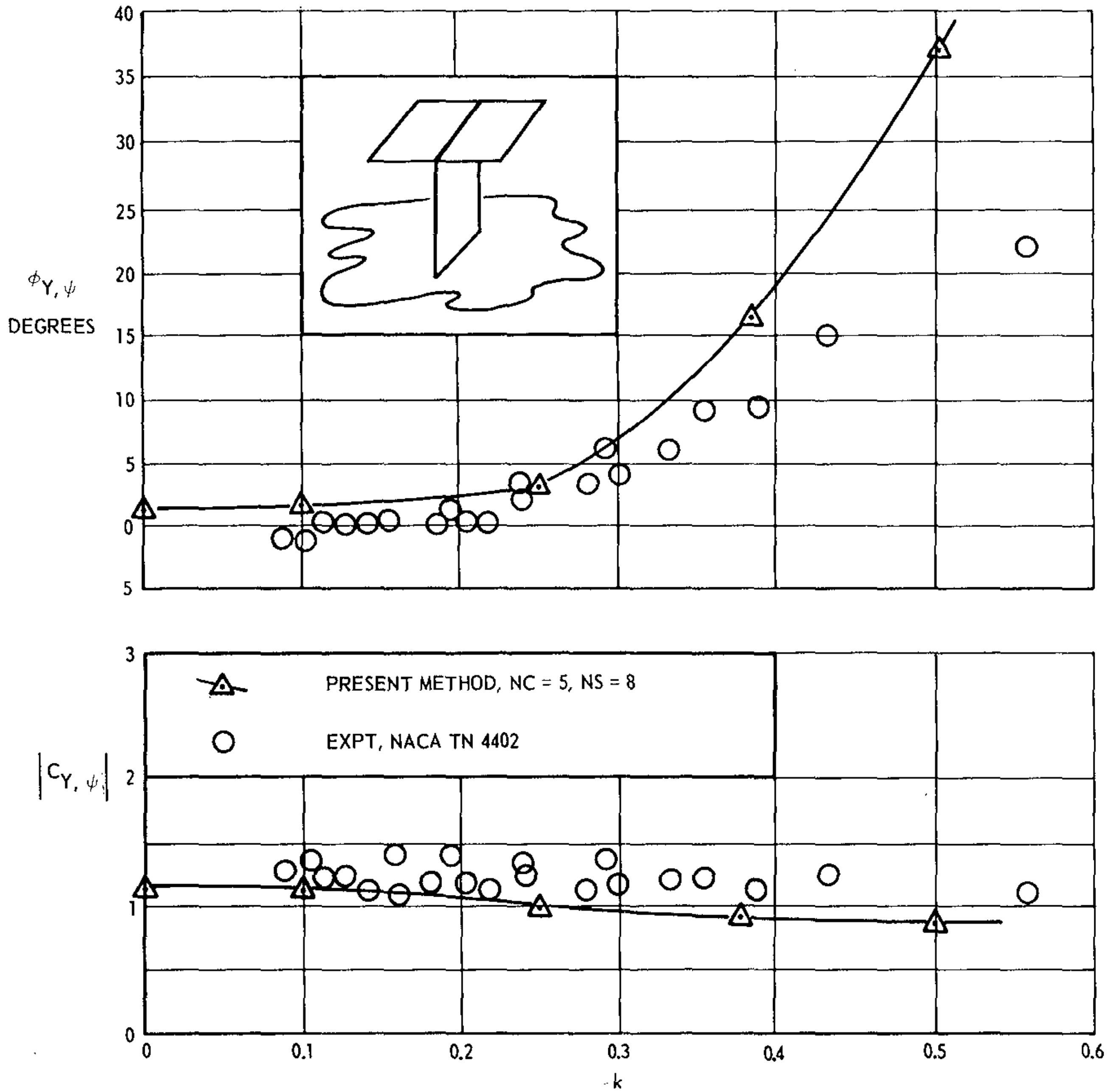

FIGURE 9 SIDE FORCE COEFFICIENT FOR T-TAIL OSCILLATING IN YAW ABOUT THE FIN MID-CHORD. $M = 0$.